**Proceedings of the ASME 34th International Conference on Ocean and Arctic Engineering
OMAE2015
May 31-June 5, 2015, St. John's, NL, Canada**

OMAE2015-41142

STEADY STATE MOTION ANALYSIS OF AN OFFSHORE WIND TURBINE TRANSITION PIECE DURING INSTALLATION BASED ON OUTCROSSING OF THE MOTION LIMIT STATE

Wilson Guachamin-Acero, Torgeir Moan, Zhen Gao
Centre of Ships and Ocean Structures (CeSOS)
Department of Marine Technology
Norwegian University of Science and Technology
Otto Nielsens veg 10, Trondheim
Email: wilson.i.g.acero@ntnu.no

ABSTRACT

Installation of Offshore Wind Turbine structural components need to be executed in sea states for which their dynamic responses are expected to remain within a safe domain or perform a limited number of outcrossings from the safe boundary beyond which the responses may lead to unsafe working conditions, large impact loads or even structural failure. A critical installation activity limiting the installation of a Transition Piece TP is often the motion monitoring phase of the mating points until its landing on the foundation. The operational limit is normally given by the horizontal displacement and the safe domain could conveniently be defined by a circle of radius r in the horizontal plane. This paper presents an existing general accurate method and its solution to estimate the outcrossing rate of dynamic responses for a circular safe boundary in short crested seas which is applicable for the motion monitoring phase of offshore wind turbine components prior to mating. The required input is calculated from spectral analysis in the frequency domain and the solution is derived for Gaussian processes. It is found that both 1^{st} and 2^{nd} order responses have to be included and that the Gaussian assumption for the slow drift motions is not valid so that its real PDF is required. Also wave spreading has large influence in the outcrossing rate and should realistically be applied. The suggested approach is in agreement with real offshore practice, and is efficient when compared with time domain simulations. Then, the outcrossing rate method could help on Marine Operations decision making during critical installation activities.

NOMENCLATURE

$S_{\eta\eta}(\omega)$ Wave spectrum
$S_X X(\omega)$ Response spectrum
$S^{(2)}_{FF}(\mu)$ Drift force spectrum
ω Wave frequency (radian)
$F^{(2)}(t)$ Second order wave force
$H_{X\eta}(\omega)$ Complex transfer function
$H_{XF}(\mu)$ Force-motion complex transfer function
T_{nm} Quadratic transfer function matrix coefficients
G_{nm} Surge, sway response matrix coefficients
λ_j Eigenvalues
$f_X(x)$ Probability density function
ρ correlation coefficient
ν^+ Outcrossing rate
J Jacobian
ϕ Normal probability density function
Φ Normal cumulative distribution function
E Expected value
m, μ Mean value
$\hat{\Sigma}$ Variance
n_X Normal unit vector
S_D Boundary between the unsafe and safe domains
PDF Probability density function
$JPDF$ Joint Probability density function
$FQTF$ Full quadratic transfer function
TP Transition Piece
MP Monopile

DAF Dynamic amplification factor
TD Time domain
HLV Heavy lift vessel
Hs Significant wave height
Tp Peak period

INTRODUCTION

According to the DNV OS H101 [3], Marine operations with reference periods less than 96 hours and planned operational periods less than 72 hours are defined as weather restricted operations. Offshore lifting operations fall within this category and therefore their planning and execution are based on weather forecast and related operational criteria (see i.e. [4]). The installation of an Offshore Wind Turbine Transition Piece TP involves several activities, each of them with their own duration, limiting parameters, safe boundaries and operational limits (see i.e. table 1). From table 1, it is observed that the total planned operational period is 13.5 hours and by adding some contingency time the reference period will be longer than the planned one. Also, after the lifting operation has started, (activity No. 4) the process cannot be interrupted until the TP has landed on the foundation (activity No. 6). From spectral analysis and with previous knowledge of the probability density functions $PDFs$ of the stochastic responses, the allowable sea states could be calculated for all activities and limiting parameters for their respective time period. Then, it could be seen that only one or a few limiting parameters will govern the complete installation. The sea states corresponding to the governing limiting parameter will result in the so called *design sea states* and together with the total reference period, suitable weather windows could be selected from the weather forecast. In many cases the forecasted sea state just complies with the *design* Hs and Tp and monitored responses. So that, a convenient tool to support the on-board decision making in Marine Operations is provided by the upcrossing (for scalar processes) and outcrossing (for vector processes) analyses, since they will provide information about how often a stochastic response will leave the safe domain or limit state function.

No.	*Activity*	*Duration* [hrs]	*Limiting parameter*	*Safe boundary*	*Oper. limit*
1	Mooring crane vessel	8	Hs	scalar limit	3m
2	Pre-lift motion monitoring	0.5	crane tip X,Y,Z	spherical radius	0.6m
3	Cut sea-fastening	1.0	roll crane barge	scalar limit	0.7deg
4	Lift-off	0.5	heave TP	scalar limit	0.5m
5	TP lowering	0.5	DAF	scalar limits	1.2
6	TP motion monitoring & mating	0.5	X,Y displ	circular radius	0.3m
7	TP heading control & leveling	2.0	wind speed	scalar limit	15m/s

TABLE 1: Sequential activities and limiting parameters for TP installation

Note: Operational limits listed above are illustrative.

FIGURE 1: Mating phase between TP and Monopile using a heavy lift offshore mono-hull crane vessel

A critical activity during the installation of an Offshore Wind Turbine TP onto a Monopile MP is often the mating phase which starts when the motions of the $TP's$ bottom (located a couple of meters over the foundation) are monitored and then lowered until it circumvents the tip of the MP (activity No. 6 in table 1, see also figure 1). Then, it is desired that the eccentricity of the connecting points during this lowering process remains smaller than the annular gap provided for installation and grouting purposes.

A practical operational limit for this activity is the horizontal displacement of the mating points and is limited by a circle with a deterministic radius r equal to the annular space. The choice of this safe boundary is rather rational than a physical approximation. Then, operational limits based on this criterion are more convenient than independent surge and sway limits where no correlation between stochastic responses are considered and extreme response distributions will lead to conservative results.

By assuming that the process is Gaussian and stationary, existing methods for outcrossing of vector processes could be applied to calculate the number of times that the TP bottom will leave the safe domain for the duration of the installation activity. Moreover 1^{st} and 2^{nd} order motions contribute to the total response and the later one generally does not follow a Gaussian distribution, and is necessary to derive its real distribution. The distribution parameters for Gaussian processes could directly be obtained from frequency domain spectral analyses and from the respective probability density functions $PDF's$ if the process is not Gaussian.

Several researchers in the past have studied the outcrossing of

vector processes and most of the work is limited to Gaussian stochastic processes, see i.e. [1], [6],[2]. Veneziano [1] presented general formulations for stationary Gaussian processes and gave solutions for elliptical and spherical domains assuming no cross-correlation between the processes and their derivatives. Exact solutions for circular domains could be obtained from existing methods. Leira [12], derived a general solution for a two dimensional vector process after solving the problem in the standard normal space and considering full correlation between the stochastic processes and their derivatives. Similarly Naess [15] presented a general method which could be applied to several stochastic variables and the solution is based on the conditional probability theory. These methods are accurate and have been compared by other researchers [8]. Also, Low [13] presented the solution for the outcrossing rate of circular safe boundary applied to the excursions of a moored vessel in extreme sea states. In this paper, the solution is given based on the Naess' [15] general method.
The solution is valid for Gaussian Processes and could directly be applied when only first order responses are relevant. Otherwise if 2^{nd} order motions contribute significantly to the total response, they should be also included and should not be considered Gaussian distributed since the results will be unconservative, see i.e. [13]. Then the probability density function *PDF* of the slowly varying part (see i.e. [16],[17],[10],[11]) is could be convoluted with the Gaussian $PDF's$ of the first order responses, so the Gaussian copula could be derived from the Nataf transformation and input in the exact solution. An important assumption made in this study is to consider that the contributions of the 2^{nd} order drift motions of the installation vessel's crane tip could be added to the 1^{st} order ones of the $TP's$ bottom. In other words it is assumed that both are independent. Other typical applications for the solutions given in here are: Tower & tripod landing on pre-installed piles, substation installation, wind turbine tower installation, control of *MP* inclination during stabbing, etc.

RESPONSE AUTO AND CROSS-SPECTRA

The distribution parameters for the stochastic responses in surge and sway and their derivatives are required to establish their $PDF's$. They could be found from spectral analysis and then assembled in covariance matrices. For Spectral analysis theory see i.e. [18], [19].
The response auto and cross response spectra for any point in the TP is defined in general:

$$S_{X_1X_2}(\omega) = H_{X_1\eta}(\omega)H^*_{X_2\eta}(\omega)S_{\eta\eta}(\omega) \tag{1}$$

Where $S_{\eta\eta}$ is the wave spectrum, X_1 and X_2 could be surge and sway displacements and the H_X are the complex transfer functions. For stationary Gaussian Processes, X_1 and its first derivative $\dot{X}_1$ are uncorrelated but not necessarily for the cross terms, the cross-spectra follow:

$$S_{X_1\dot{X}_2}(\omega) = i\omega H_{X_1\eta}(\omega)H^*_{X_2\eta}(\omega)S_{\eta\eta}(\omega) \tag{2}$$

For the derivative of the stochastic processes, the response spectrum reads:

$$S_{\dot{X}_1\dot{X}_2}(\omega) = \omega^2 S_{X_1X_2}(\omega) \tag{3}$$

The covariance coefficients follows directly from the integration of the response spectra.

$$\sigma_{X_1X_2} = Re\int_0^\infty S_{X_1X_2}(\omega)d\omega \tag{4}$$

The second order contributions could be taken from the crane vessel, so that the response spectra could be calculated from the drift force spectrum $S_F^{(2)}$ and the coupled two degree of freedom force-motion transfer function matrix H_{XF} for surge and sway as shown in equation (9). It can be found to be (see i.e. [9]).

$$S^{(2)}_{X_1X_2}(\mu) = \sum_{k=1}^{2}\sum_{l=1}^{2} H_{X_1F_k}(\mu)H_{X_2F_l}(\mu)^* S^{(2)}_{F_kF_l}(\mu) \tag{5}$$

The cross spectra of the wave drift forces could be calculated from the wave spectrum $S_{\eta\eta}(\omega)$ and the complex quadratic transfer function coefficients $T_{k,l}$. The difference frequency is defined as $\mu = \omega_j - \omega$:

$$\begin{aligned} S^{(2)}_{F_kF_l}(\mu) = 8\int_0^\infty S_{\eta\eta}(\omega)S_{\eta\eta}(\omega+\mu)\times \\ T_k(\omega,\omega+\mu)T_l^*(\omega,\omega+\mu)d\omega \end{aligned} \tag{6}$$

Then, the covariance matrices could be calculated and added to the one due to first order motions assuming that both are independent. The spectrum of slow drift velocities could be treated in the same way. The 1^{st} order motions follow a Gaussian distribution, similarly the combined 1^{st} and 2^{nd} order velocities have a near-Gaussian behavior [13] due to the small contribution from the slowly varying components (see also table 4 for the study case response statistics). In contrast, the 2^{nd} order drift motions of the crane vessel will not follow a Gaussian distribution and its real *PDF* is required. In the following, the *PDF* of the drift motions of the crane vessel are calculated based on the method proposed by Naess [15] which has been applied by other researchers, see i.e [10],[11],[13], [20]. After that, the combined probability density function is calculated as the convolution of the 1^{st} and 2^{nd} order $PDF's$. Finally the Nataf transformation will provide the equivalent Gaussian copula to be input in the outcrossing rate equation.

PDF of the 1^{st} and 2^{nd} order surge and sway motions

The 2^{nd} order wave force acting on a vessel in any degree of freedom and heading could be written in the time domain as follows, (see i.e. [16],[10]).

$$F^{(2)}(t) = \sum_{n=1}^{N}\sum_{m=1}^{N} Q_{nm}\hat{u}_n\hat{u}_m^* exp\left[i\left(\omega_n - \omega_m\right)t\right] \tag{7}$$

Where $\hat{u}$ is a complex Gaussian random variable and:

$$Q_{nm} = \left(T_{nm}^c - iT_{nm}^s\right)\sqrt{2S_{\eta\eta}\left(\omega_n\right)\Delta\omega}\sqrt{2S_{\eta\eta}\left(\omega_m\right)\Delta\omega} \tag{8}$$

In equation (8) T_{nm}^c and iT_{nm}^s are the real and imaginary parts of the second order transfer function coefficients. In this paper, the full Quadratic Transfer Function $FQTF$ is applied.
A crane barge could be modeled as a linear mass spring and damper system in surge and sway with the following force-motion transfer function matrix (contributions from the other degrees of freedom are not included in the calculations only for simplicity):

$$H_{XF} = \begin{bmatrix} H_{X_1F_1} & H_{X_1F_2} \\ H_{X_2F_1} & H_{X_2F_2} \end{bmatrix} \tag{9}$$

From equation (8)and (9) a motion response square matrix $\mathbf{G}$ of dimension $N\times N$ could be assembled where the coefficients have the following form i.e. for surge.

$$G_{nm}^{x_1} = \begin{bmatrix} H_{X_1F_1} & H_{X_1F_2} \end{bmatrix}\begin{bmatrix} Q_{nm}^{x_1} \\ Q_{nm}^{x_2} \end{bmatrix} \tag{10}$$

The Eigenvalues from matrix $\mathbf{G}$ denoted as λ_j could be sorted such that $\lambda_j, j = 1,2,..M$ are positive and $\lambda_j, j = M+1,..N$ are negative. The probability density function is found to be (see i.e. [16], [10]):

$$f_{X^{(2)}}(x) = \left| \begin{array}{ll} \sum_{j=1}^{M} \frac{\mu_j}{\lambda_j} exp\left(-x/\lambda_j\right) & x \geq 0 \\ \sum_{j=M+1}^{N} \frac{\mu_j}{|\lambda_j|} exp\left(-x/\lambda_j\right) & x < 0 \end{array} \right. \tag{11}$$

Where:

$$\mu_j = \prod_{\substack{k=1\\k\neq j}}^{N}\left[1-\lambda_k/\lambda_j\right]^{-1} \tag{12}$$

The previous described procedure could also be applied to random short-crested seas for which case each frequency contribution is to be replaced by a sum over all wave directions at that frequency, a more detailed study is found in [17] and the formulations given above are still valid.
The combined probability density function is calculated as the convolution of the 1^{st} and 2^{nd} order $PDF's$ which could be evaluated numerically using i.e. Matlab functions.

$$f_X(x) = \int_{-\infty}^{\infty} f_{X^{(1)}}(x - x^{(2)}) f_{X^{(2)}}(x^{(2)}) dx^{(2)} \tag{13}$$

Where, $X^{(1)}$ and $X^{(2)}$ are the first and second order motion vectors.

Nataf Transformation

From equation (13) the Gaussian copula for the marginal $PDF's$ and covariance matrix could be derived via the Nataf transformation. The joint PDF for surge and sway is given by:

$$f_X(x_1,x_2) = \phi_2(y_1,y_2,\rho'_{12})|J| \tag{14}$$

Where, $\phi_2(y_1,y_2,\rho'_{12})$ is the normal $JPDF$ with zero mean values, unit standard deviations and correlation coefficient ρ'_{12}. The Jacobian of the Transformations J follows:

$$|J| = \frac{f_{x_1}(x_1)f_{x_2}(x_2)}{\phi(y_1)\phi(y_2)} \tag{15}$$

Where f_{X_i} and $\phi(y_i)$ are the marginals and the corresponding normal standard $PDF's$. The correlation coefficient could be evaluated numerically and iteratively from the known normalized random variables $Z_i = (X_i - \mu_{X_i})/\sigma_{X_i}$ and correlation coefficient ρ_{12} to satisfy the following equation:

$$\rho_{12} = \int_{-\infty}^{\infty}\int_{-\infty}^{\infty} z_1 z_2 \phi_2(y_1,y_2,\rho'_{12}) dy_1 dy_2 \tag{16}$$

OUTCROSSING OF VECTOR PROCESSES

The exact solution for the outcrossing rate could be determined from the Rice's formula whose solution for Gaussian processes and circular safe boundary could be established.

Multivariate Gaussian Joint PDF

A multivariate Gaussian probability density function is given as follows, see i.e. Hearn et al [7].:

$$f_X = \frac{1}{(\sqrt{2\pi})^n|\Sigma_X|^{1/2}} exp\left[-\frac{1}{2}\left(X - m_X\right)^T {\Sigma_X}^{-1}\left(X - m_X\right)\right] \tag{17}$$

Where for a bivariate PDF $n=2$, Σ is the covariance matrix of the stochastic responses and correspondingly m_X is the vector of the mean values.

Marginal distribution parameters

For a multivariate joint Gaussian density function of several processes and their derivatives, the distribution parameters are:

$$f_{\dot{X}X}(\dot{X},X) = N(\mu,\Sigma) \tag{18}$$

$$\mu = \left\{ \begin{matrix} \mu_{\dot{X}} \\ \mu_X \end{matrix} \right\}; \Sigma = \begin{bmatrix} \Sigma_{\dot{X}\dot{X}} & \Sigma_{\dot{X}X} \\ \Sigma_{X\dot{X}} & \Sigma_{XX} \end{bmatrix} \tag{19}$$

Where Σ_{XX}, $\Sigma_{\dot{X}X}$ and $\Sigma_{\dot{X}\dot{X}}$ are the covariance matrix for the stochastic responses, the covariance matrix of the responses and their derivatives (being zero for the diagonal terms) and the covariance matrix for the derivatives of the responses. The moments for the conditional velocity distribution are given as follows:

$$f_{\dot{X}|X}(\dot{X}|X) = N(\hat{\mu}_{\dot{X}|X},\hat{\Sigma}_{\dot{X}|X}) \tag{20}$$

$$\begin{aligned} \hat{\mu}_{\dot{X}|X} &= \mu_{\dot{X}} + \Sigma_{\dot{X}X}\Sigma_{XX}^{-1}(X-m_X) \\ \hat{\Sigma}_{\dot{X}|X} &= \Sigma_{\dot{X}\dot{X}} + \Sigma_{\dot{X}X}\Sigma_{XX}^{-1}\Sigma_{X\dot{X}} \end{aligned} \tag{21}$$

For a two dimensional vector process, the conditional mean velocity vector and covariance matrix are respectively:

$$\hat{\mu}_{\dot{x}_n|X} = \left\{ \begin{matrix} \hat{\mu}_{\dot{x}_1} \\ \hat{\mu}_{\dot{x}_2} \end{matrix} \right\} \tag{22}$$

$$\hat{\Sigma}_{\dot{x}_n|X} = \begin{bmatrix} \hat{\Sigma}_{\dot{x}_1\dot{x}_1} & \hat{\Sigma}_{\dot{x}_1\dot{x}_2} \\ sym & \hat{\Sigma}_{\dot{x}_2\dot{x}_2} \end{bmatrix} \tag{23}$$

Outcrossing rate

The outcrossing frequency of a boundary S_D between a safe and unsafe domains is given by the Rice's formula, see i.e. Melchers [14]

$$\nu_{S_D}^{+} = \int_{S_D} dx \int_0^{\infty} \dot{x}_n f_{\dot{X}_n X}(\dot{x}_n, x) d\dot{x}_n \tag{24}$$

Where, $\dot{x}_n$ is the product of its normal and the derivative of the vector process so that they depend on the actual position on the surface. Instead of the $JPDF$ from equation (24) is is better to express it in terms of conditional probability density functions.

$$\nu_{S_D}^{+} = \int_{S_D} \int_0^{\infty} \dot{x}_n f_{\dot{X}_n}(\dot{x}_n|X=x) d\dot{x}_n f_X(x) dx \tag{25}$$

Outcrossing rate based on Naess' method

Naess [15] gave a general solution based on the properties of the conditional probability. Here, formulations given from equations (17-25) are applicable. Based on his formulation, the limit state function defined by a circle could be written in the following form:

$$D(X) = \left(\frac{x_1}{r}\right)^2 + \left(\frac{x_2}{r}\right)^2 = 1 \tag{26}$$

The gradient of the reliability function then results:

$$\dot{D}(X) = n_{x_1}\dot{x}_1 + n_{x_2}\dot{x}_2 \tag{27}$$

Where the unit normal velocity components are identified as:

$$n_{\dot{X}} = \left\{ \begin{matrix} n_{\dot{x}_1} \\ n_{\dot{x}_2} \end{matrix} \right\} = \left\{ \begin{matrix} 2x_1/r^2 \\ 2x_2/r^2 \end{matrix} \right\} \tag{28}$$

Also, x_1 could be written in the following form:

$$x_1 = \pm r(d - x_2/r)^{0.5} \tag{29}$$

Using results from equations (22&23) the mean and variance of the conditional distribution for the mean velocity in equation (25) is calculated as follows:

$$m_{\dot{x}_n} = \hat{\mu}_{\dot{x}_1} n_{x_1} + \hat{\mu}_{\dot{x}_2} n_{x_2} \tag{30}$$

The variance of the normal velocity reads:

$$\sigma_{\dot{x}_n}^2 = \hat{\Sigma}_{\dot{x}_1\dot{x}_1} n_{x_1}^2 + \hat{\Sigma}_{\dot{x}_2\dot{x}_2} n_{x_2}^2 + 2[\hat{\Sigma}_{\dot{x}_1\dot{x}_2} n_{x_1} n_{x_2}] \tag{31}$$

For Gaussian processes, the inner integral in equation (25) could be found to be:

$$\begin{aligned} E(\dot{x}_n|X=x) = \int_0^{\infty} \dot{x}_n f_{\dot{X}_n} d\dot{x}_n = \sigma_{\dot{x}_n} exp \\ \left[-\frac{1}{2}\left(\frac{m_{\dot{x}_n}}{\sigma_{\dot{x}_n}}\right)^2\right] + m_{\dot{x}_n}\Phi\left(\frac{m_{\dot{x}_n}}{\sigma_{\dot{x}_n}}\right) \end{aligned} \tag{32}$$

Using equations (17&32), equation (25) gives:

$$\nu_{S_D}^{+} = \int_{x_2} E\left(\dot{x}_n | X = x\right) f_X\left(x_1 = f(x_2, d), x_2\right) |J| dx_2 \qquad (33)$$

$$J = \frac{2r}{\left[h - (x_2/r)^2\right]^{0.5}} \qquad (34)$$

Equation 33 could be evaluated numerically and $|J|$ is the Jacobian of the transformation of x_1 in the bivariate PDF and should be evaluated for $d = 1$ following the definition of the limit state function.

STUDY CASE: INSTALLATION OF A TP USING AN OFFSHORE CRANE BARGE

The dynamic model used in the analysis is composed of a heavy lift crane barge and a TP hanging from the crane tip for a condition corresponding to the motion monitoring phase. The outcrossing rate will be calculated based on the equations given above followed by TD simulation for some cases.

Structures main particulars

The main particulars of the structures are given in table 2 and a model setup is shown in figure 2.

Parameter	*Notation*	*Value*	*Units*
- Crane barge			
Displacement	∇	5.95E4	Ton
Length	L	180	m
Breadth	B	37	m
Draught	T	10	m
Roll nat. period	T_{n_4}	11.6	s
- Transition Piece			
Mass	M	200	Ton
Length	L	23	m
Diameter	D	6.4	m

TABLE 2: Main particulars of structures

Distribution parameters

The response distribution parameters are calculated from spectral analysis using the AQWA FER program and the corresponding drift motion PDF as described before. The environmental parameters and simulation cases are shown in tables 3.

The wave spreading function is modeled according to the cos^n function (see [5]). Table 4 summarizes the required input for the outcrossing analyses which has been elaborated using formulations given in equations (1-13) and are shown only for Environmental condition 1. Based on table 4, the covariance matrices could be assembled using the combined terms in the last column of table 4. At this stage, the outcrossing rate could be evaluated using equation equation (33) by assuming that the second order motions follow a Gaussian distribution and the results are shown in figure 4. However this assumption may not be applicable; in figure 3 the $PDF's$ corresponding to the slow varying motions of the barge's crane tip, the first order Gaussian responses of the $TP's$ bottom and the one resulting from their convolution are plotted.

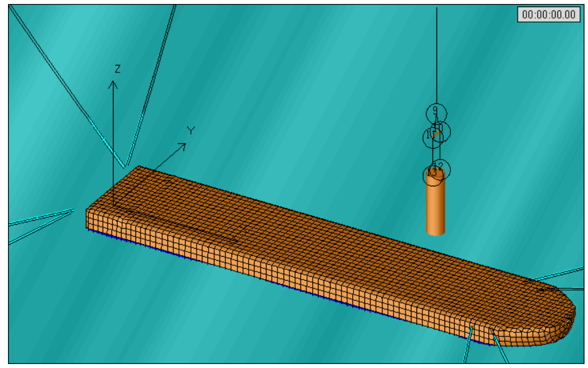

FIGURE 2: Coupled dynamic model for TP installation

Environmental condition	*Wave Spec*	*Hs* [m]	*Tp* [s]	*Gamma* [-]	*Dir* [deg]
1	JONSWAP	1.0	7.5	1.2	15
2	JONSWAP	1.5	6.5	1.2	180, 135, 90

TABLE 3: Environmental conditions
Note: Wave directions are given counterclockwise from stern

Table 5 shows a summary of the statistical moments for the $PDFs$ plotted in figure 3. Note that it is convenient to shift the responses to zero mean values, (see Table 4) which allow us to have the reference system at the origin of the circle; otherwise the limit state function will have to be defined with respect to the global axis reference system.

Outcrossing rate

The solution of the problem is found numerically by dividing the circular perimeter for each r into a sufficient number of segments to achieve accurate results; here a total number of 61 line segments is chosen. The outcrossing rate is then calculated for the exact solution for Gaussian approximation given in equation (33) and the environmental conditions given in table 3.

Parameter	*Units*	*Sim. case*	*Descirption*	1^{st} *order*	2^{nd} *order*	*combined*
-TP bottom response						
σ_{x_1}	m	1	long crested& FQTF	6.71E-2	3.78E-2	7.70E-2
		2	short crested: n=4& FQTF	8.07E-2	2.79E-2	8.54E-2
		3	short crested: n=8& FQTF	7.33E-2	3.00E-2	7.92E-2
		4	short crested: n=16& FQTF	6.90E-2	3.16E-2	7.59E-2
σ_{x_2}	m	1	long crested& FQTF	5.39E-2	8.00E-3	5.44E-2
		2	short crested: n=4& FQTF	9.79E-2	1.80E-2	9.95E-2
		3	short crested: n=8& FQTF	6.79E-2	1.34E-2	6.92E-2
		4	short crested: n=16& FQTF	5.45E-2	1.05E-2	5.57E-2
$\rho_{x_1 x_2}\sigma_{x_1}\sigma_{x_2}$	m^2	1	long crested& FQTF	1.60E-3	6.33E-5	1.66E-3
		2	short crested: n=4& FQTF	1.27E-3	9.03E-5	1.41E-3
		3	short crested: n=8& FQTF	1.75E-3	8.69E-5	1.88E-3
		4	short crested: n=16& FQTF	1.83E-3	9.46E-5	1.95E-3
$\sigma_{\dot{x}_1}$	m/s	1	long crested& FQTF	5.29E-2	4.00E-3	5.30E-2
		2	short crested: n=4& FQTF	6.06E-2	1.62E-2	6.27E-2
		3	short crested: n=8& FQTF	5.54E-2	1.92E-2	5.87E-2
		4	short crested: n=16& FQTF	5.28E-2	2.29E-2	5.75E-2
$\sigma_{\dot{x}_2}$	m/s	1	long crested& FQTF	3.61E-2	1.00E-3	3.61E-2
		2	short crested: n=4& FQTF	6.11E-2	9.61E-3	6.18E-2
		3	short crested: n=8& FQTF	4.43E-2	7.78E-3	4.49E-2
		4	short crested: n=16& FQTF	3.69E-2	6.47E-3	3.74E-2
$\rho_{\dot{x}_1\dot{x}_2}\sigma_{\dot{x}_1}\sigma_{\dot{x}_2}$	m^2/s^2	1	long crested& FQTF	7.00E-4	1.97E-5	9.26E-4
		2	short crested: n=4& FQTF	6.09E-4	2.26E-5	6.32E-4
		3	short crested: n=8& FQTF	8.06E-4	2.16E-5	8.27E-4
		4	short crested: n=16& FQTF	8.18E-4	2.33E-5	8.42E-4
$\rho_{\dot{x}_1 x_2}\sigma_{\dot{x}_1}\sigma_{x_2}$	m^2/s	1	long crested& FQTF	2.77E-4	5.44E-6	2.82E-4
		2	short crested: n=4& FQTF	1.79E-4	-4.18E-5	1.37E-4
		3	short crested: n=8& FQTF	-8.63E-5	-3.75E-5	-1.24E-4
		4	short crested: n=16& FQTF	-1.59E-4	-3.86E-5	-1.98E-4
$\rho_{x_1\dot{x}_2}\sigma_{x_1}\sigma_{\dot{x}_2}$	m^2/s	1	long crested& FQTF	-2.77E-4	-5.44E-6	-2.82E-4
		2	short crested: n=4& FQTF	-1.79E-4	4.18E-5	-1.37E-4
		3	short crested: n=8& FQTF	8.63E-5	3.75E-5	1.24E-4
		4	short crested: n=16& FQTF	1.59E-4	3.86E-5	1.98E-4
$m_{x_1}, m_{x_2}, m_{x_3}$	m	1-4		0	0	0
$m_{\dot{x}_1}, m_{\dot{x}_2}, m_{\dot{x}_3}$	m/s	1-4		0	0	0

TABLE 4: Distribution parameters for environmental condition 1, JONSWAP Hs=1.0m, Tp=7.5sec, $\alpha = 15deg$, $\gamma = 1.2$

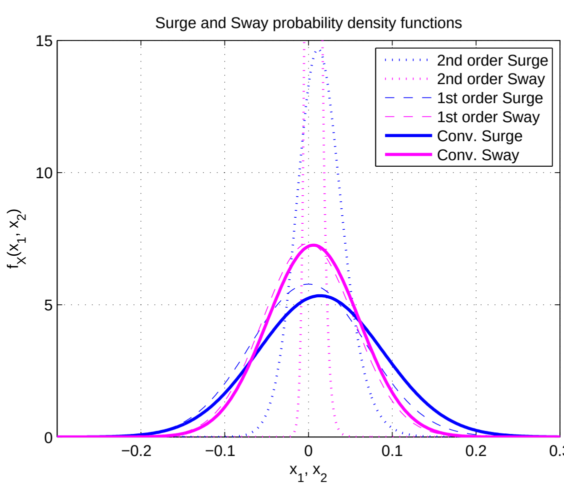

FIGURE 3: Convolution of 1^{st} and 1^{nd} order motion $PDF's$ for case 4

Distribution	*mean*	*variance*	*skewness norm.*	*kurtosis norm.*
- SURGE				
1^{st}*order*	0	0.0048	0	3
2^{nd}*order*	0.0145	0.0008	0.2962	3.6187
combined	0.0145	0.0056	0.0170	3.0106
- SWAY				
1^{st}*order*	0	0.0030	0	3
2^{nd}*order*	0.0060	0.0001	0.5532	4.1838
combined	0.0060	0.0030	0.0013	3.0003

TABLE 5: Statistical moments for probability density functions for case 4

For the second order motion Gaussian assumption, the results are plotted in figure 4. Next, the second order motion $PDF's$ are obtained from equation (11) which are then convoluted with the first order Gaussian probability density functions and transformed into the Gaussian copula via the Nataf transformation; after a few iterations the correlation coefficient from equation (16) is determined. This approach here is referred here as *Ana-*

lytical method and is applied to the rest of simulation cases. The results are shown in figure 4. An example of TD simulations for

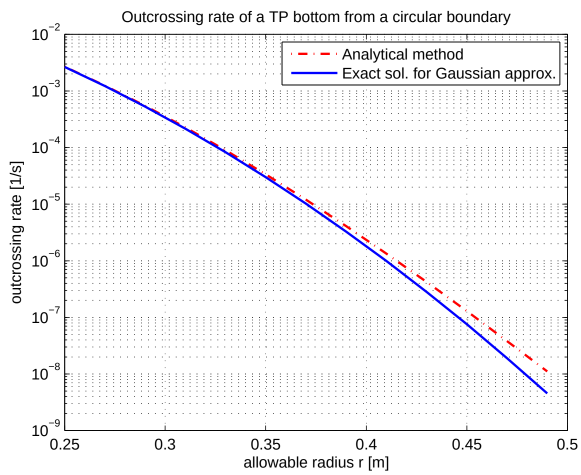

FIGURE 4: Outcrossing rate of a circular boundary for case 4 (n=16). JONSWAP Hs=1.0m, Tp=7.5sec, α=15deg, γ=1.2

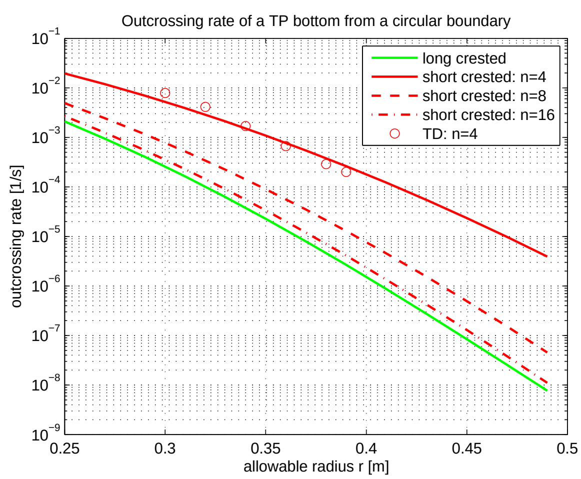

FIGURE 5: Outcrossing rate for a circular boundary for long and short crested seas using FQTF (cases 1-4). JONSWAP Hs=1.0m, Tp=7.5sec, α=15deg, γ=1.2

the excursions of the bottom of the TP for both long and short crested seas are given in figures 6 and 7 respectively, where the allowable radius of the safe domains is $r = 0.26m$ and the total simulation time is $t = 3000s$. A large difference is observed in the number of outcrossings and is consistent with the averaged results shown in figure 5. Moreover the correlation between the responses is different and the effect of first order motions becomes more important for short crested seas. Similarly for the

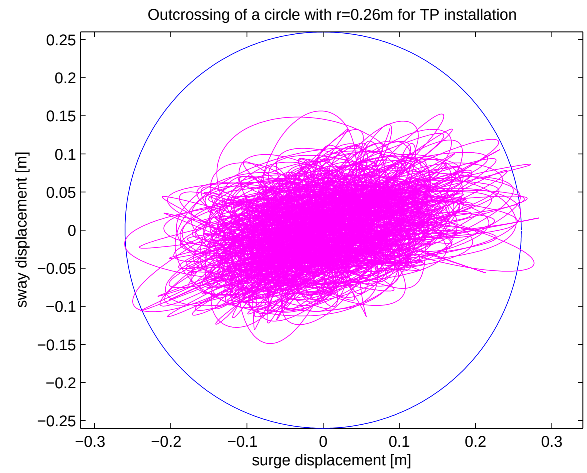

FIGURE 6: Outcrossings from a circular domain of radius r=0.26m and t=3000s. Case 1: long crested seas. JONSWAP Hs=1.0m, Tp=7.5sec, α=15deg, γ=1.2

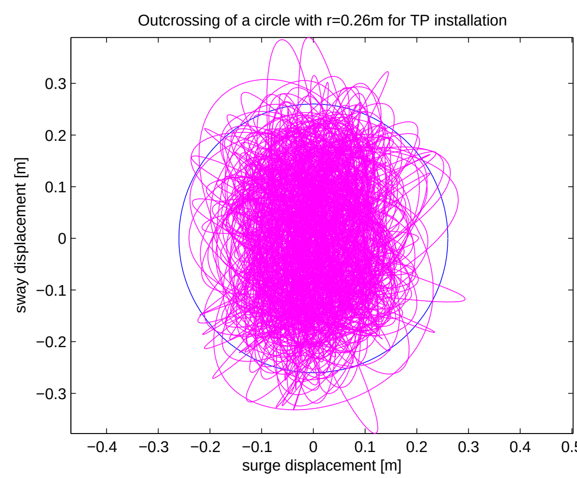

FIGURE 7: Outcrossings from a circular domain of radius r=0.26m and t=3000s. Case 2: short crested seas (n=4). JONSWAP Hs=1.0m, Tp=7.5sec, α=15deg, γ=1.2

environmental condition No.2 in table 3 the influence of wave direction and spreading are calculated for head, quartering and beam seas and plotted in figure 8.

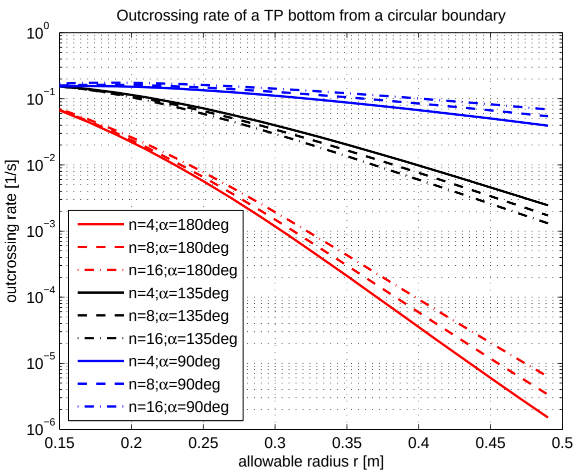

FIGURE 8: Outcrossing rate for a circular boundary for head, bow-quartering and beam short-crested seas. JONSWAP Hs=1.5m, Tp=6.5sec, γ=1.2

Analysis of Results

From figure 3 and table 5, it is observed that the second order $PDF's$ should not be considered as Gaussian since the extremes will be underestimated due to the significant difference in tail of the distributions, especially when slow drift motions give significant contribution to the total responses. Also, figure 4 shows that the Gaussian approximation may lead to unconservative results especially when second order motions are dominating. From figures 5& 8 it is observed that directional wave spectra will have large influence on the time variant random processes when analyzing the responses of floating structures and should preferably be used for modeling marine operations. Also in figure 10 it is seen that the assumption made in this paper may not always hold if the pendulum motion of the TP could be affected by the the 2^{nd} order responses of the barge's crane tip since they may not be totally independent. This fact explains the small differences in the slowly varying surge motions of the crane barge and TP and it makes the assumption questionable especially if the drift motions are large and their natural frequencies higher (see also TD results in figure 5). In this study the natural period in surge and sway are 57 and 52 sec respectively (corresponding to a ship with 8 point mooring lines each with 500KN pre-tension) while the pendulum period is 17 sec and the results may still be acceptable. Additionally, it could also be seen that wave spreading has large influence on the outcrossing rate because floating vessels are sensitive to wave heading (see figures 5 & 8). As expected, the results for long crested seas will approach the ones for short crested seas for large values of n. From figure 8 and head waves the outcrossing rate for short crested ($n = 4$) is lower than for long crested seas ($n \approx 16$) because the 2^{nd} order motions are dominating. In contrast for beam seas, long crested waves give larger outcrossing rates since first order responses dominate. Slowly varying drift motions should be included in the analyses, and the limiting parameters and safe boundaries should account for them. Figure 9 which is a typical example of response spectra for surge and sway for simulation *cases 1 & 2* shows not only significant differences at both drift and wave frequencies but also for long and short crested seas.

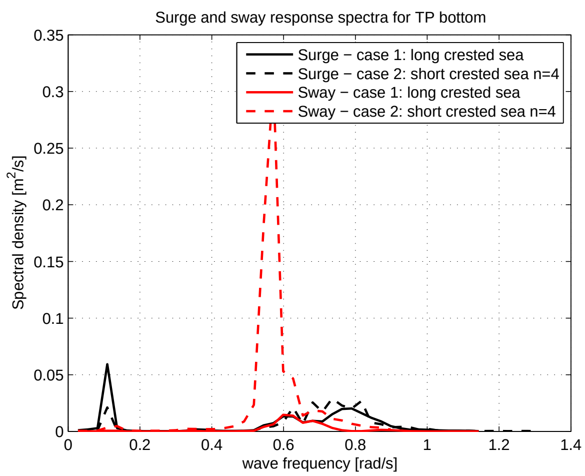

FIGURE 9: Surge and sway response spectra for typical *cases*1&2, JONSWAP Hs=1m, Tp=7.5sec, α=15deg,$\gamma = 1.2$

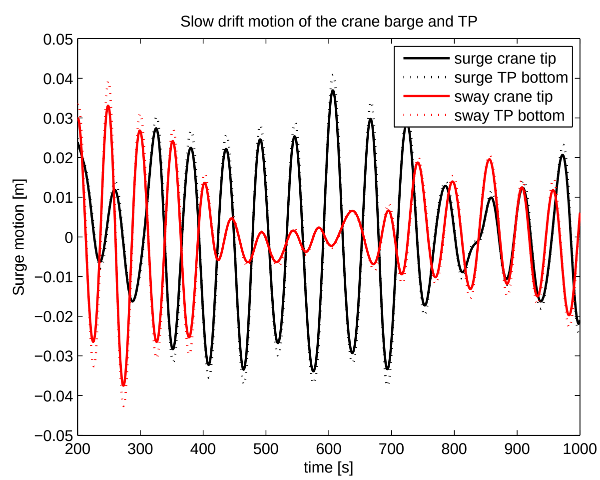

FIGURE 10: Time domain history for the slow drift motions of the crane tip and TP bottom *case*2, Hs=1.0m, Tp=7.5sec, α=15deg,γ=1.2. (Mean values are shifted to zero).

CONCLUSIONS AND RECOMMENDATIONS

Outcrossing rates of safe boundaries could be used to better assess safety during critical offshore installation activities. The procedure described in this paper could be applicable especially for installation phases such as mating and landing; however it is necessary to first verify the independence assumption between first and second order responses. Wave spreading is important and has to be included when the installation is executed with floating crane barges. The computational costs are very low and can vary from a few seconds to a few minutes depending on how fine the grids are selected for the spectral and Eigenvalue analyses. When deriving the second order motion $PDF's$ a convergence criteria could be set based on the spectral analysis results. Whenever available, $2D$ forecasted wave spectra based on frequency and direction parameters should be used. They will not only reduce uncertainties in the wave spreading angle but will also allow a more realistic description of multimodal wave spectra which is preferred when analyzing responses of floating structures (including wind turbine concepts) and the allowable responses are small. Numerical integration problems may be encountered when carrying out the Eigenvalue analysis for head and beam seas for symmetric bodies. They may be solved by slightly changing the heading and integration range of the motion vectors. In Offshore wind turbine installation the allowable motion responses are small and therefore should be calculated in a more realistic and accurate manner.

ACKNOWLEDGMENTS

This work has been financially supported by the Research Council of Norway granted through the Department of Marine Technology and the Centre of Ships and Ocean Structures *CeSOS* from the Norwegian University of Science and Technology *NTNU*.

REFERENCES

[1] M. Grigoriu D. Veneziano and C. A. Cornell. Vector-process models for system reliability. *Journal of the Engineering Mechanics Division*, EM3:441–460, 1977.

[2] O. Ditlevsen. Guassian outcrossings from safe convex polyhedrons. *Journal of the Engineering Mechanics*, 109:127–148, 1983.

[3] DNV-OS-H101. *Marine Operations, General.* , 2011.

[4] DNV-OS-H205. *Lifting Operations.* , 2014.

[5] DNV-RP-C205. *Environmental Conditions and Environmental Loads.* , 2010.

[6] O. Hagen. Conditional and joint failure surface crossings of stochastic processes. *Engineering Mechanics*, 118(9):1814–1839, 1992.

[7] G. Hearn and A. Metcalfe. *Spectral analysis in Engineering*. Elsevier Ltd., 2004.

[8] H. Jia and T. Moan. Comparative realiability analysis of ships under vector-load processes. *Marine Science and Technology*, 14(485-498), 2009.

[9] R. S. Langley. Second order frequency domain analysis of moored vessels. *Journal of the Applied Ocean Research*, 9(1):7–18, 1987.

[10] R. S. Langley. A statistical analysis of low frequency second-order forces and motions. *Journal of the Applied Ocean Research*, 9(3):163–170, 1987.

[11] R. S. Langley and S. McWilliam. A statistical analysis of first and second order vessel motions induced by waves and wind gusts. *Journal of the Applied Ocean Research*, 15:13–23, 1993.

[12] B. Leira. *Gaussian vector-processes for Reliability analysis involving wave-induced load effects*. PhD thesis, Institut for Marine Konstruksjoner NTH, 1987.

[13] Y. M. Low. Efficient vector outcrossing analysis of the excursion of a moored vessel. *Probabilistic Engineering Mechanics*, 24:565–576, 2009.

[14] R. Melchers. *Structural Reliability Analysis and Prediction*. John Wiley and Sons, 2002.

[15] A. Naess. Prediction of extremes of morison-type loading-an example of a general method. *Ocean Engineering*, 10:313–324, 1983.

[16] A. Naess. The statistical distribution of second-order slowly-varying forces and motions. *Journal of the Applied Ocean Research*, 8(2):110–118, 1986.

[17] A. Naess. Statistical analysis of nonlinear, second-order forces and motions of offshore structures in short-crested random seas. *Probabilistic Engineering Mechanics*, 5(4):192–203, 1990.

[18] A. Naess and T. Moan. *Stochastic Dynamics of Marine Structures*. Cambridge University Press, 2013.

[19] D. Newland. *An introduction to Random Vibrations, Spectral and Wavelet Analysis*. Dover Publications, 2005.

[20] C. T. Stansberg. A simple method for estimation of extreme values of non-guassian slow-drift responses. In *International Offshore and Polar Engineering Conference*, pages 442–451, 1991.